

Devitrification and recrystallization of magnetic glass $\text{La}_{0.5}\text{Ca}_{0.5}\text{MnO}_3$

P. Chaddah, Kranti Kumar, and A. Banerjee

UGC-DAE Consortium for Scientific Research (CSR), University Campus, Khandwa Road, Indore 452 017, India

(Received 3 December 2007; revised manuscript received 18 January 2008; published 10 March 2008)

We report studies on a magnetic glass formed by the arrest of the ferromagnetic-metallic to antiferromagnetic-insulating transition in a manganite around half doping, $\text{La}_{0.5}\text{Ca}_{0.5}\text{MnO}_3$. The observed glass-to-crystal conversion rate varies drastically and nonmonotonically with temperature; this variation is qualitatively consistent with what we predict by phenomenology. We also show that both homogeneous and heterogeneous nucleation can be obtained in the same sample under different annealing conditions. This gives rise to a gigantic change in resistivity without application of any magnetic field.

DOI: 10.1103/PhysRevB.77.100402

PACS number(s): 75.30.Kz, 64.60.My, 64.70.P-, 75.47.Lx

Glasses form when kinetics is arrested below a temperature T_g , preserving the high-temperature structure while avoiding the first-order liquid-solid transformation at T_C . The inequality between the free energies of the two phases changes sign at T_C , but because of the free energy barrier separating the two phases, the low-temperature ordered phase may actually form only when the fluctuation energy in the disordered phase is sufficient to overcome this free energy barrier.¹ If heterogeneous nucleation is inhibited by the absence of seeds for nucleation, then the supercooled state persists below T_C , and homogeneous nucleation takes place only when the free energy barrier reduces to $\sim kT$ in the neighborhood of the supercooling limit T^* . The kinetics of this transformation process can get arrested for $T_g > T^*$ when the liquid is metastable (see the schematic in Fig. 1). Then, the supercooling of the high-temperature phase can seamlessly lead to the kinetically arrested glass phase if heterogeneous nucleation is prevented. Such systems where slow cooling of samples free of nucleating sites produces glass is known in glass formers such as *ortho*-terphenyl.² Further cooling will retain the kinetically arrested glass state even while lowering the temperature below T^* , where the free energy barrier has disappeared (see the schematic in Fig. 1). The lack of dynamics in this kinetically arrested state helps retain the liquid structure in a temperature regime where its free energy is unstable and prevails over thermodynamics. In such cases, splat cooling or even rapid cooling is not needed for glass formation. The unstable glass retaining the liquid structure can also be obtained when T_g is lower than T^* , but rapid cooling is necessary with the time for cooling being much shorter than the finite time required for the structural rearrangement accompanying crystallization. Such behavior with $T_g < T^*$ is noted in metallic glasses.³

We now consider what happens as the glass is warmed from well below T_g to just above T_g in these two cases, i.e., for $T_g > T^*$ and $T_g < T^*$. In the case where $T_g < T < T^*$, kinetics is restored to a state that is unstable in that there is no barrier in free energy, and the “glass” rapidly converts to the crystalline solid. The conversion rate is dictated by the kinetics and will be faster as temperature is raised since kinetics is faster at higher temperatures. If the temperature T is raised above T^* before devitrification is complete (this applies also in the case where $T_g > T^*$), kinetics is restored to a state that is now metastable. No devitrification or rapid conversion to the crystalline solid would occur because there is now a bar-

rier in free energy. A slow conversion would be seen due to thermal activation over the barrier, and the conversion rate is dictated by the height of this free energy barrier, the conversion is now slower at higher T since the barrier rises rapidly with rising T .⁴ We shall show later from time decay measurements these contrasting temperature dependences, but the glass we study belongs to the recently discovered family of “magnetic glasses”⁵ described below.

Arrest of kinetics can also inhibit a first-order field (H)

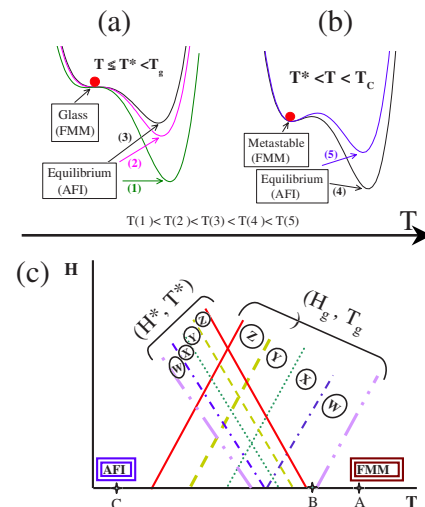


FIG. 1. (Color online) Evolution of free energy as a function of T and the heuristic H - T diagram for a first-order FMM to AFI transition below the T_C . (a) shows the free-energy landscapes for $T \leq T^*$, and its evolution with increasing T is shown from 1 to 3. In a situation when $T \leq T^* < T_g$, the high-temperature phase (FMM) is frozen as glass in an unstable state (without a barrier). (b) shows the energy barrier separating the metastable state from the equilibrium state increases with T , as shown for cases 4 and 5. (c) The anticorrelated broadened (H^*, T^*) and (H_g, T_g) bands are represented by four regions, viz., W , X , Y , and Z . While cooling, if a region encounter the corresponding (H_g, T_g) before it crosses the respective (H^*, T^*) , then it will get arrested in the high- T FMM phase and remain as a glassy phase down to the lowest T . The overlap of the bands at $H=0$ indicates that there is some arrested FMM phase even when the system is cooled in $H=0$. Cooling in higher field will render larger fractions as an arrested FMM phase. The significance of points A , B , and C are discussed in the text.

and temperature induced transition where both the phases on either side of the transition have a long-range structure, including magnetic order. It has been shown recently that many disorder-broadened first-order magnetic transformations are interrupted by a glasslike arrest of kinetics. These materials range from colossal magnetoresistance (CMR) manganites,^{6–10} to magnetocaloric materials^{11–13} and other intermetallics,^{5,14,15} and offer advantages in studying the behavior of glasses. Here, T_C and T^* vary rapidly with H , and relative positions of T_g and T^* can be changed by cooling in one value of H and warming in another value of H . By slow cooling the sample in a value of H where $T_g > T^*$, and then isothermally varying H at T well below T_g , we can have a glass at any other field H^\dagger (including that for which $T_g < T^*$) without having to take recourse to rapid cooling. Through this protocol, a glass can form during slow cooling when $T_g > T^*$, but devitrifies when $T_g < T^*$ on heating.^{9,12} Further, the broad transition presents a situation where a glasslike unstable or metastable state (Fig. 1) coexists with a crystallinelike equilibrium state.^{5–12}

The first-order transition temperature (T_C) in such systems will, because of the intrinsic disorder, have a distribution of values over regions having a dimension of the order of correlation length. The first-order field and temperature induced transitions are broadened with respect to the control variables like H and T resulting in the (H_C, T_C) line being broadened into a band.^{16,17} The spinodal lines corresponding to the limit of supercooling (H^*, T^*) and corresponding to the limit of superheating (H^{**}, T^{**}) would also be broadened into bands.⁶ Each of these bands corresponds to a quasicontinuum of lines; each line corresponds to a region of the disordered sample with a length scale of the order of the correlation length. If kinetic arrest were to occur below a (H_g, T_g) line in the pure system, the disordered system would have a (H_g, T_g) band formed out of the quasicontinuum of (H_g, T_g) lines. Each line would again correspond to a local region of the sample. If the lines in each of these bands correspond to different regions of the sample, one can seek a correlation between the position of a line in the (H_g, T_g) band and the position of the corresponding (i.e., from the same region) line in the (H^*, T^*) band. An anticorrelation has been proposed between T_g and T^* ,¹⁸ which is experimentally verified in many such magnetic transitions,^{6,8–10,12,14} where regions with higher T_g have lower T^* .

Another advantage in studying these materials to understand metastable behavior arises from T_g being different (just like T_C or T^*) for different regions of the sample. This “broadening” of T_g offers a situation where $T_g > T^*$ for some regions (at a given H) but not for other regions. In the schematic in Fig. 1(c), the anticorrelation reported earlier between T_g and T^* bands is invoked and we show a case where the highest T_g is above the homogeneous nucleation T^* . The regions with higher T_g are arrested when we cool because homogeneous nucleation has not yet taken place at T_g and remain in the high- T “liquid” phase, while the regions with lower T_g transform to the equilibrium phase before their kinetics is arrested because their T_g is below their T^* . If this “coexisting phase” is now warmed above T_g (but below T_C), the fraction of the coexisting phases is maintained. On a

second cooldown from this intermediate annealing temperature $T_a < T_C$, the already transformed phase acts like nucleating seeds. The regions that did not undergo homogeneous nucleation during the first cooldown can now undergo heterogeneous nucleation well above T^* and, thus, above their T_g . We shall show later that both homogeneous and heterogeneous nucleation can be obtained in the same sample under different annealing conditions.

A polycrystalline $\text{La}_{0.5}\text{Ca}_{0.5}\text{MnO}_3$ sample has been prepared through a well-established chemical route known as “pyrophoric method.” High purity (>99.9%) La_2O_3 , CaCO_3 , and $\text{C}_4\text{H}_6\text{MnO}_4 \cdot \text{H}_2\text{O}$ are taken in stoichiometric quantities as starting materials. These materials are dissolved in aqueous nitric acid, and the resulting solutions are mixed together with triethanolamine. The complex solution is heated to dehydrate and decompose, leaving behind organic-based, black fluffy precursor powder. This dried mass is then ground to fine powder, pelletized, and then calcined at 1000 °C for 3 h in oxygen atmosphere. The powder x-ray diffraction (XRD) was carried out using an 18 kW Rigaku Rotaflex RTC 300 RC diffractometer with $\text{Cu } K_\alpha$ radiation. A Rietveld profile refinement of XRD pattern confirms that the sample is in single phase without any detectable impurity and crystallizes in orthorhombic structure with a $pnma$ space group. The resistivity and magnetic measurements are performed using commercial setups (14 T physical property measurement system vibrating sample magnetometer (PPMS-VSM), M/s Quantum Design, USA). All the temperature variations are done at the fixed rate of 1.5 K/min.

Figure 2(a) shows the magnetization as a function of temperature measured in 1 T field under various protocols. The hysteresis between field-cooled cooling (FCC) and field-cooled warming (FCW) paths indicates a disorder-broadened first-order transition from ferromagnetic-metallic (FMM) to antiferromagnetic-insulating (AFI) with reducing temperature. However, a substantial magnetization in the low-temperature antiferromagnetic phase, similar to Ref. 19, suggests the persistence of ferromagnetic phase. Based on the measurements similar to those reported earlier in the glasslike kinetically arrested magnetic systems,^{6,8–12} we propose that the AFI state is in equilibrium at low temperature and the FMM phase fraction exists as the nonergodic kinetically arrested glassy state.²⁰ We can collect larger fractions of a glasslike arrested FMM phase at 5 K by cooling in a 6 T field and then reducing the field to 1 T.^{6,9,10} This glasslike arrested FMM state devitrifies on heating, as depicted in Fig. 2 by the rapid fall in magnetization (of the 6 T cooled state), which approaches the equilibrium AFI phase while warming. This half-doped manganite should have the spin-aligned value of $3.5\mu_B/\text{Mn}$ accompanied by metallic conductivity.¹⁹ The observed 1 T fcc magnetization of $0.61\mu_B/\text{Mn}$ at 5 K can be attributed to a frozen FMM phase fraction of about 17%, which is close to the percolation threshold for electrical conductivity. Hence, around this FMM phase fraction, the drastic resistivity (R) changes are a more sensitive tool, compared to the magnetization, to probe small changes in the phase fractions. Figure 2(b) shows the heating and cooling cycles of the zero-field resistivity. Apart from the expected thermal hysteresis, the decrease in resistivity with the decrease in temperature below 70 K (this is clearer in Fig. 4)

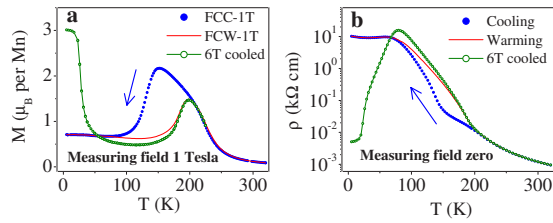


FIG. 2. (Color online) Temperature dependence of magnetization in 1 T field and resistivity in zero field of $\text{La}_{0.5}\text{Ca}_{0.5}\text{MnO}_3$ measured under different protocols. (a) M vs T while cooling (FCC) in a 1 T field from 320 to 5 K and again while warming (FCW) from 5 K shows the thermal hysteresis accompanying the first-order ferromagnetic to antiferromagnetic transition. After cooling the sample in a 6 T field, the field is reduced isothermally to 1 T at 5 K and M is measured while warming. The large value of M at 5 K reflects a dominant arrested ferromagnetic phase, and its devitrification starts at around 20 K. (b) R vs T while cooling in a zero field from 320 to 5 K and again while warming from 5 K shows the thermal hysteresis accompanying the first-order metallic to insulating transition. After cooling the sample in the 6 T field, the field is reduced isothermally to zero at 5 K and R is measured while warming. The low value of R at 5 K reflects a large fraction of arrested metallic phase, and its devitrification starts at around 20 K.

reflects the presence of the FMM phase fraction in the AFI matrix. Similar to magnetization, the zero-field resistivity also shows a larger fraction of FMM phase when the sample is cooled in 6 T (Fig. 2(b)). Different values of magnetization and resistivity in the same measurement temperature (5 K) and field (1 T for magnetization and zero for resistivity) indicate the presence of nonergodic states. The concomitant sharp decrease in magnetization and the increase in resistivity of the 6 T cooled state around 20 K, as shown in Figs. 2(a) and 2(b), result when this arrested nonergodic FMM phase devitrifies to the AFI phase on warming.⁹

To study the evolution of this FMM glass, we measured resistivity as a function of time at different temperatures. During cooldown from 320 to 5 K in 1 T, $\approx 17\%$ of the sample has a frozen metallic fraction, whose $T_g > T^*$. This glassy fraction remains invariant when the field is isothermally reduced to zero at 5 K. The sample is then heated to the measurement temperature, and resistivity is measured as a function of time for 2 h. Following this procedure, the time dependence of resistivity is measured at different temperatures, but in Fig. 3, we show only a few of them for clarity. Resistance rises more rapidly with time as the measurement temperature is increased from 60 to 80 K. This is consistent with the kinetics being faster at higher temperature and the above phenomenology of free energy barrier being negligible at both temperatures (see Fig. 1(a)). The time evolution of resistance at 100 K is much slower and decreases further as the temperature is raised to 110 K and higher. This is consistent with the above phenomenology that at 100 K and above, the FMM glass fraction is left in a local minimum of free energy, and excitation over the free energy barrier is required to convert it to the equilibrium AFI phase (see Fig. 1(b)). The barrier rises sharply^{1,4} as temperature is raised above 100 K, and the increased barrier dictates a slower conversion even though the thermal energy is more. Thus, we

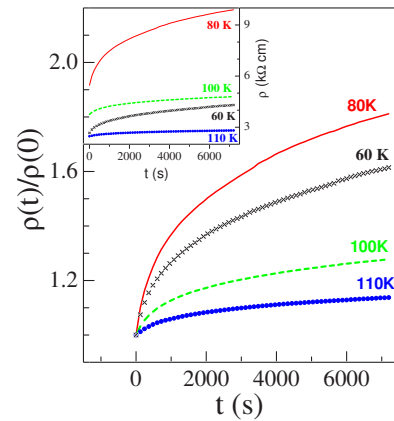


FIG. 3. (Color online) Time dependence of resistivity at different temperatures for the $\text{La}_{0.5}\text{Ca}_{0.5}\text{MnO}_3$ sample. For measurement at each temperature, the sample is cooled in a 1 T field from 320 to 5 K. Then, the field is isothermally reduced to zero, and the sample is warmed to the respective T . The main panel shows the evolution of R after it is normalized to the respective values of R at $t=0$. The inset shows the evolution of R in absolute units.

infer that $80 \text{ K} < T^* < 100 \text{ K}$ in zero field, which is consistent with the data shown in Fig. 2 and also reported elsewhere.²⁰ We may note that the actual starting values of resistivity at 100 K lies between those at 60 and 80 K (inset of Fig. 3), ruling out any artifacts having dominated the time-evolution measurements.

Figure 4 shows the resistivity measurement in zero field. The inset shows the thermal hysteresis across the first-order FMM to AFI phase while cooling from 320 to 5 K and again heating from 5 K. However, in this cooling process, the complete transformation to the AFI state has not taken place even after approaching the lowest temperature. This is evident from the main panel of Fig. 4 where instead of heating all the

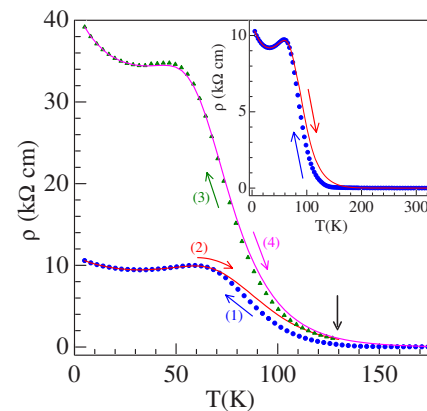


FIG. 4. (Color online) Resistivity of $\text{La}_{0.5}\text{Ca}_{0.5}\text{MnO}_3$ in zero field while cooling from 320 K (path 1). Then, R is measured while warming to 130 K (path 2) and cooling to 5 K (path 3) followed by warming all the way to 320 K (path 4). The sharply rising resistivity after warming to 130 K is a consequence of the additional AFI phase formed by heterogeneous nucleation. The inset shows complete thermal cycling between 320 and 5 K measured after completion of the four paths shown in the main panel, bringing out the first-order transition.

way from 5 to 320 K the sample is heated up to 130 K and cooled back again to 5 K. A spectacular increase in resistivity takes place, giving rise to about four times increase in resistivity at the lowest temperature. We understand this as follows. As shown in Fig. 1(c), when the sample is cooled in zero H toward point A , we have a homogeneous FMM phase even though it is metastable. At point A , the entire sample is above the supercooling spinodal and no homogeneous nucleation takes place during the first cooling. Since regions corresponding to the W band get kinetically arrested at point B , before there is any homogeneous nucleation, these regions remain FMM at the lowest temperature of point C . However, regions corresponding to bands X , Y , and Z have been converted to AFI at point C since their respective spinodal T^* is higher than their corresponding T_g . We now warm the sample toward point B . We retain regions corresponding to X , Y , and Z bands in the AFI phase, but the region corresponding to the W band is kinetically arrested in the FMM phase. Lowering the temperature from 60 K, for example, just retraces the resistivity measured during the first cooldown from 320 K. We now warm toward point A . The region corresponding to the W band is no longer kinetically arrested, and as evident from the data and the earlier discussion, at 130 K it is above its supercooling spinodal and is in a metastable state [corresponding to the situation of Fig. 1(b)]. It is, however, now sitting in an environment where many nuclei of the AFI phase exist corresponding to bands X , Y , and Z . There is now a possibility for the FMM phase of band W to undergo heterogeneous nucleation and convert to the AFI phase. This is what we observe during the second cooling from 130 K when we observe a drastic enhancement of resistivity, and thus of the AFI fraction, at 5 K. It is clear that this heterogeneous nucleation required seed nuclei of the AFI phase, and these AFI nuclei convert back to FMM and

disappear if we heat the sample to 320 K. Cooling again from 320 K (inset of Fig. 4) reproduces the lower resistance of the first cooling corresponding to homogeneous nucleation and also ruling out microcracks as the cause of increased resistance observed in the previous cycle.

In this Rapid Communication, we have studied one example of the recently discovered magnetic glasses to establish two experimental features. We have shown that devitrification occurring when $T_g < T < T^*$ is more rapid as T rises, consistent with there being no free-energy barrier surrounding the glass state and the kinetics dictating the conversion rate. If, however, $T_g > T^*$, then the glass state has a free-energy barrier surrounding it. Conversion to the equilibrium state is now slower as T is raised because the barrier height dictates the conversion rate. Thus, we clearly show that the La-Ca-Mn-O around half-doping contains a glasslike FMM phase coexisting with the equilibrium AFI phase at low temperature even when cooled in zero field. Moreover, this glasslike FMM phase can convert to the equilibrium AFI phase both by the processes of devitrification or recrystallization. Furthermore, we have also shown that both homogeneous and heterogeneous nucleations can be obtained in the same sample under different annealing conditions. This gives rise to a gigantic change in resistivity even in zero field for a CMR manganite, $\text{La}_{0.5}\text{Ca}_{0.5}\text{MnO}_3$, sample. The functionality of CMR manganite arises from a considerable change in resistivity at the same temperature when a magnetic field is applied. In the present system, gigantic change in resistivity arises from only thermal cycling without any magnetic field. Thus, only temporary heating to two different temperatures can give rise to a big change in resistivity. As a first step, it can act as a thermal switch.

The DST Government of India is acknowledged for funding the 14 T PPMS-VSM.

- ¹P. M. Chaikin and T. C. Lubensky, *Principles of Condensed Matter Physics* (Cambridge University Press, Cambridge, 1994).
- ²S. Brawer, *Relaxation in Viscous Liquids and Glasses* (The American Ceramic Society, Inc., Columbus, OH, 1985).
- ³A. L. Greer, *Science* **267**, 1947 (1995).
- ⁴P. Chaddah and S. B. Roy, *Phys. Rev. B* **60**, 11926 (1999).
- ⁵M. K. Chattopadhyay, S. B. Roy, and P. Chaddah, *Phys. Rev. B* **72**, 180401(R) (2005), and references therein.
- ⁶Kranti Kumar, A. K. Pramanik, A. Banerjee, P. Chaddah, S. B. Roy, S. Park, C. L. Zhang, and S.-W. Cheong, *Phys. Rev. B* **73**, 184435 (2006).
- ⁷W. Wu, C. Israel, N. Hur, P. Soonyong, S.-W. Cheong, and A. De Lozane, *Nat. Mater.* **5**, 881 (2006).
- ⁸A. Banerjee, K. Mukherjee, Kranti Kumar, and P. Chaddah, *Phys. Rev. B* **74**, 224445 (2006).
- ⁹A. Banerjee, A. K. Pramanik, Kranti Kranti, and P. Chaddah, *J. Phys.: Condens. Matter* **18**, L605 (2006).
- ¹⁰R. Rawat, K. Mukherjee, Kranti Kumar, A. Banerjee, and P. Chaddah, *J. Phys.: Condens. Matter* **19**, 256211 (2007).
- ¹¹S. B. Roy, M. K. Chattopadhyay, P. Chaddah, J. D. Moore, G. K. Perkins, L. F. Cohen, K. A. Gschneidner, Jr., and V. K. Pechar-sky, *Phys. Rev. B* **74**, 012403 (2006).
- ¹²S. B. Roy, M. K. Chattopadhyay, A. Banerjee, P. Chaddah, J. D. Moore, G. K. Perkins, L. F. Cohen, K. A. Gschneidner Jr., and V. K. Pechar-sky, *Phys. Rev. B* **75**, 184410 (2007).
- ¹³V. K. Sharma, M. K. Chattopadhyay, and S. B. Roy, *Phys. Rev. B* **76**, 140401(R) (2007).
- ¹⁴Pallavi Kushwaha, R. Rawat, and P. Chaddah, *J. Phys.: Condens. Matter* **20**, 022204 (2008).
- ¹⁵S. B. Roy and M. K. Chattopadhyay, *EPL* **79**, 47007 (2007).
- ¹⁶A. Soibel, E. Zeldov, M. Rappaport, Y. Myasoedov, T. Tamegai, S. Ooi, M. Konczykowski, and V. Geshkenbein, *Nature (London)* **406**, 282 (2000).
- ¹⁷S. B. Roy, G. K. Perkins, M. K. Chattopadhyay, A. K. Nigam, K. J. S. Sokhey, P. Chaddah, A. D. Caplin, and L. F. Cohen, *Phys. Rev. Lett.* **92**, 147203 (2004).
- ¹⁸P. Chaddah, A. Banerjee, and S. B. Roy, arXiv:cond-mat/0601095 (unpublished).
- ¹⁹J. C. Loudon, N. D. Mathur, and P. A. Midgley, *Nature (London)* **420**, 797 (2002).
- ²⁰A. Banerjee, Kranti Kumar, and P. Chaddah, arXiv:0711.2347 (unpublished).